



# Differential Equation for Turbulence Power Losses and Energy Spectra Based on Consolidated Empirical Results

H. E. Schulz<sup>†</sup>

*Hydro-Engineering Solutions (Hydro-LLC), Auburn, AL, 36830, U.S.A.*  
*Department of Civil and Environmental Engineering, Auburn University, Auburn, AL, 36830, U.S.A*

<sup>†</sup>Corresponding Author Email: [hschulz@hydro-engineering.net](mailto:hschulz@hydro-engineering.net); [hschulz@sc.usp.br](mailto:hschulz@sc.usp.br)

(Received December 13, 2021; accepted April 15, 2022)

## ABSTRACT

A second order differential equation for the energy dissipation rate of turbulence is presented. The derivation procedure is explained. The obtained governing equation is a Euler equation, which integration naturally conduces to power laws for the energy dissipation rate as a function of the wavenumber, a result that is extended to the energy spectrum of turbulence. Power laws are obtained for the cases of two equal and two different real roots. For the case of two conjugate complex roots, the solution is a sum of sine and cosine functions of the normal logarithm of the wavenumber. The differential equation accrues from a more basic equation obtained through thermodynamic-type steps that joint part of already consolidated empirical and semi-empirical information on turbulence existing in the literature, and is formally analogue to the Thermodynamics equation of thermal radiation. It is also shown that parameters of turbulence like length and velocity scales may be related to this formulation.

**Keywords:** Turbulence spectra; Thermodynamic analogy; Euler differential equation; Empirical laws; Constitutive equations.

## NOMENCLATURE

$\mathcal{A}$	coefficient of the 5/3 law	$r_{1,2}$	exponents of Euler equation solutions
$C_{1,2}$	integration constants	$S$	entropy
$D$	diameter	$\mathcal{S}_{A...D}$	integration constants
$E(k)$	turbulence energy spectrum	$T$	temperature
$E(k)_N$	normalized spectrum	$T_{1,2}$	integration constants
$\dot{E}$	power per unit mass times volume	$u$	energy per unit volume
$f$	friction factor	$\dot{u}$	power dissipation per unit volume
$g$	gravity acceleration	$\dot{U}$	power dissipation
$G_{1...7}$	auxiliary coefficients	$V$	velocity scale
$h_\ell$	head loss	$\mathcal{V}$	volume
$IJ$	unknown coefficient of Euler equation	$x$	turbulent transfer coefficient (mass)
$k$	wavenumber	$\alpha, \beta, \delta$	auxiliary coefficients
$k_N$	normalized wavenumber	$\varepsilon$	characteristic power dissipation
$k_{C1, C2}$	lower and upper cutoff wavenumbers	$\varepsilon(k)$	spectrum of power dissipation
$k_D$	dissipative wavenumber	$\theta_{1...4}$	auxiliary coefficients
$k_E$	energy containing wavenumber	$\nu$	viscosity
$KE$	kinet energy per unit mass	$\Xi$	integration constant
$k_R$	reference wavenumber	$\rho$	fluid density
$\ell$	eddy diameter	$\phi$	joining empirical information function
$L$	length	$\psi$	joining empirical information function
$\dot{Q}$	flow rate	$\omega_{1,2}$	real and imaginary parts of $r_{1,2}$
$\bar{Q}$	heat		

## 1. INTRODUCTION

Turbulence studies have the characteristic of using sophisticated mathematical concepts like statistical differential equations and spectral analyses; together with *ad hoc* propositions (see [Monin and Yaglom, 1979, 1981](#)), usually implemented in numerical codes, like the turbulent viscosity and its relation with higher order statistical moments in the  $k$ - $\varepsilon$  and the large eddy models; or the law of the wall used as boundary condition and applied in numerical meshes close to solid boundaries (see [Pope 2000](#)). The examples may be enriched with other *ad hoc* equations that resume the sound empirical knowledge acquired along about one and half centuries of investigations solving turbulent flows (taking as initial reference the name ‘‘Turbulence’’ given by the future Lord Kelvin in 1887, see for example [Schmitt 2017](#)). Correlations for heat and mass transfer, and for drag coefficients; the Chézy equation for channel flows; the Darcy-Weisbach equation for head losses; the 5/3 law and additional power laws for the turbulence energy spectrum; the different scales of turbulence, are among the empirical knowledge used to complete theoretical studies on turbulence ([Brodkey 1967](#); [Brodkey and Hershey 1988](#)).

In the first stage of the investigations, evidently the equations derived from empirical observations were linked to the specific phenomenon under study. In this sense, for example, the Darcy-Weisbach equation and the 5/3 law for the spectrum of turbulence are results obtained for different questions generated in independent (at that time) sectors of fluid dynamics. The same comparison can be made for studies on heat and mass transfer coefficients and spectral distributions.

In a second stage of the investigations, the existence of a large amount of empirical and semi-empirical information for different aspects of turbulence induces to explore at least part of this practical knowledge to locate eventual links, allowing generating a more encompassing empirical or constitutive formulation of turbulence. This may be understood as the natural way to advance in the comprehension of inner-connections between empirical parameters and concepts in any field of study, being the present stage of the studies in turbulence. It is not meant that new empirical information is not more generated, but that the different conclusions induce to search for connections among them. An example of such approach may be found in [Badillo and Matar \(2017\)](#).

Studies on turbulence use tools and concepts that can be considered similar to some used in Thermodynamics (spectra are one example). Similarly to what happens presently in the field of turbulence, the variables, concepts, laws, and general features of Thermodynamics were proposed and lapidated along a long time. About three and half centuries were necessary to have the present consistent theoretical structure, which also began through independent studies (considering as initial reference date the peri-od around 1650, when Otto von Guericke conceived and built his vacuum pump,

as mentioned for example by [Selvi and Sugumar, 2018](#)). Similarities between equations of both fields are shown in this study. Considering their derivation, ideal conditions are common: isothermal, isentropic, irreversible conditions are examples in Thermodynamics, while stationarity, isotropy (statistical properties with spherical symmetry), are examples in turbulence, and are also assumed here.

In the case of isotropic turbulence, when using the spectral description ([Hinze 1959](#)), there is a simple relation between the mean velocity scale  $V$  and the energy spectrum  $E(k)$ , given by:

$$\frac{3}{2}V^2 = \int_0^\infty E(k)dk \quad (1)$$

The variable  $k$  is the wavenumber, defined as the inverse of the eddy diameter  $\ell$ :

$$k = \frac{1}{\ell} \quad (2)$$

Isotropic turbulence also furnishes a simple relation between the power dissipation per unit mass  $\varepsilon$ , the fluid kinematic viscosity  $\nu$ , and the energy spectrum ([Hinze 1959](#)), in the form:

$$\varepsilon = 2\nu \int_0^\infty k^2 E(k)dk \quad (3)$$

The integrations of Eqs. (1) and (3) are performed along the whole positive range of wavenumbers, for which the evolution of the energy spectrum with the wavenumber must be known. However, a definitive equation of  $E(k)$  is still not disposable. A possible option would be to obtain  $E(k)$  from a previous knowledge of  $\varepsilon(k)$ , the energy dissipation rate as a function of  $k$ , also still not disposable. Considering a generic turbulent flow occurring in a volume of finite extent, the size of the eddies (or the length of turbulent motions) is restricted at both large and small extremes. The maximum possible length is given by a characteristic dimension of the volume occupied by the fluid, and the minimum possible length is given by the extent of the stable viscous movement. From Eq. (2), these dimensions also furnish cut-off or limiting wavenumbers, shortly indicated by  $k_{C1}$  (lower  $k$ ) and  $k_{C2}$  (upper  $k$ ).

To have functions of  $k$ , integrations in the range of  $k_{C1}$  to  $k$ , and of  $k$  to  $k_{C2}$ , where  $k$  is a generic wavenumber, may be used (instead of the whole positive  $k$  axis). This procedure allows studying how spectra and other variables vary with  $k$ . Positive and negative signs are obtained according to the adopted limits (ranges) of integration.

The statistical/mathematical treatment of turbulence with its physical principles is well documented in the literature. Decades of contributions are adequately exposed, discussed, and organized, so that a body of knowledge of the theme is accessible to present and future researchers. In this sense, the equations of conservation of mass, momentum, and energy; the use of mean operators; the generation of statistical moments of ever higher orders (the closure problem of statistical turbulence); the isotropic case; the spectral analyses; the solutions for specific

conditions; and so on, form the basis of mathematical tools, concepts and procedures for further expected mathematical advances (Hinze 1959; Monin and Yaglom 1979, 1981; Pope 2000, for example).

Further, as mentioned, the existing empirical and semi-empirical information help solving intricate problems usually formulated numerically, and allow explaining the still convenience of turbulence ‘models’ through *ad hoc* definitions of macro and microscales. These semi-empirical scales show that the number of nodes in 3D direct simulations grows with the 9/4<sup>th</sup> power of the Reynolds number, quickly becoming excessively time and power consuming. The codes themselves are built following well established rules to linearize nonlinear problems, and using general discretization schemes. The environment of the numerical codes thus also relies on a solid mathematical basis (Patankar, 1980, Rodi, 2000; Pope, 2000; Hanjalić, 2006; Rebollo and Lewandowski, 2014; Layton, 2018, for example).

On the other hand, the knowledge generated by each experimental observation is the fact, the undeniable reality that must be followed by any theoretical proposal or numerical code that intends to explain that specific turbulence phenomenon. In a resumed way, specific experimental data are needed to bound models by reality.

The previous three paragraphs show that the basic physical principles expressed in mathematical form, together with the numerical tools, compose the natural way for the studies in turbulence. However, the needed empirical information still seems to be a set of independent conclusions, not necessarily related to each other. In this sense, there is still “space” to work on the mathematization of consolidated independent empirical results, so that at least part of them can be systematized and linked to a common formulation. It is in this “space” or “gap region” that this study was conducted.

This text initially reports a procedure to obtain a formulation that encompasses a number of empirical observations and results inherent to turbulence. The procedure uses known relevant physical variables (like the power dissipation), a set of variables for which a link is searched (similar to  $E(k)$ ,  $\nu$ ,  $\varepsilon$ ,  $k$ , of the dimensional/power law analysis of Onsager (1945) on the Kolmogoroff’s 1941 theory), and results of experimental studies in turbulent transfer phenomena. The procedure does not use regression analyses on sets of data, but brings together already established equations combining their different information. Time consuming trial-and-error calculations were conducted when more than one functional form seemed adequate to build up the formulation, selecting the best suited. The original empirical information can be extracted back from the final formulation through usual mathematical operations (Schulz 2001).

Further, this text uses the obtained formulation to propose an integrable second order governing differential equation for the power dissipation  $\varepsilon$  in turbulent flows. The solutions of its integration are

used to also obtain energy spectra, which allow justifying observed power laws with different exponents. Still further, the text shows that usual length and velocity scales are also linked to the proposed formulation.

## 2. PROPOSED FORM OF THE EQUATION

This section resumes and complements the formulation that links empirical conclusions in turbulence which was presented in a less developed form by Schulz (1991, 2001). It was originally a review procedure of existing empirical equations intending to reduce the amount of information of the different work hypotheses usually linked to them. As starting variable, the power dissipation  $\dot{U} = \dot{u}\mathcal{V}$  was chosen because it is a key parameter in most of the turbulence quantification found in the literature. It was divided here by the density  $\rho$  of the fluid furnishing  $\dot{E} = \dot{U}/\rho = \dot{u}\mathcal{V}/\rho = \varepsilon\mathcal{V}$ , which differential form is:

$$d\dot{E} = \varepsilon d\mathcal{V} + \mathcal{V}d\varepsilon \tag{4}$$

$\dot{U}$  is the power dissipation,  $\dot{u}$  is the power dissipation per unit volume,  $\varepsilon$  is the power dissipation per unit mass, and  $\mathcal{V}$  is the volume of fluid under analysis, including the dissipation scales. Further, following Onsager’s (1945) contribution to Kolmogoroff (1941) and Obukhoff (1941) studies, who suggested a constitutive equation between the variables  $\varepsilon$ ,  $k$ ,  $\nu$  and  $E(k)$  based on dimensional/power law grounds, an auxiliary function  $\phi$  was also proposed having the following functional dependence:

$$\phi = \phi(\varepsilon, \mathcal{V}, x) \tag{5}$$

Equation (5) is a variation of the Onsager’s suggestion. Turbulence increases the transfer of physical properties like heat, momentum, mass, and kinetic energy, being  $x$  the parameter that quantifies turbulent transfer. In general, the more turbulent the fluid, the more transfer increases, thus increasing  $x$ , which may be viewed as a measure of turbulence. It substitutes the viscosity  $\nu$ , which quantifies the transfer of momentum in laminar shear movements, not being a measure of turbulence. The volume  $\mathcal{V}$  and the wave- number  $k$  are related through  $\mathcal{V} = \pi/6k^3$  for isotropic turbulence, both thus carrying geometrical information of the turbulent movement.  $\phi$  is not defined, a different condition of  $E(k)$  used by Onsager (1945), already known. The differential form of Eq. (4) served as basis to conveniently express Eq. (5) also in differential form (Schulz 1991, 2001), which for the present notation is given by:

$$d\phi = (\alpha x^\beta)\varepsilon d\mathcal{V} + (x^\delta)\mathcal{V}d\varepsilon \tag{6}$$

The convenience is given by the similarity between Eqs. (4) and (6), the first with a clear physical meaning. Taking  $\alpha=1$  and  $\beta=\delta=0$  reproduces Eq. (4), which would imply  $\phi=\dot{E}$ . Evidently, more general results were aimed. The first part of this study was thus directed to obtain exponents  $\beta$  and  $\gamma$  that quantify the effects of  $x$  in each parcel, and the coefficient  $\alpha$  that quantifies the weight of each

parcel in Eq. (6) based on empirical results of the literature. A definition for  $d\phi$  followed as consequence of this analysis. The second part of the study was directed to the application of the resulting equation to obtain related turbulence spectra.

For comparison, the [Onsager's \(1945\)](#) procedure involves a dimensional analysis with  $\varepsilon$ ,  $k$ ,  $\nu$  and  $E(k)$  that results in three nondimensional variables, which are then conveniently related through a product of powers of two of them. This convenient choice quantifies  $E(k)$  as the product of powers of  $\varepsilon$  and  $k$ , corroborated experimentally.

**2.1 Defining Adequate  $\alpha$ ,  $\beta$ , and  $\gamma$**

One of the most used tools for calculating power dissipation in closed and open conduit is the empirical Darcy-Weisbach equation (see, for example, [White, 2016](#)). It already unifies information of power dissipation, velocity and length scales for unidirectional mean turbulent flows, being thus interesting for the present formulation. For tubes the Darcy-Weisbach and the power dissipation equations are, respectively (see [White 2016](#)):

$$h_\ell = f \frac{L V^2}{D 2g} \tag{7a}$$

$$\dot{U} = \rho g Q h_\ell \tag{7b}$$

$V$  is the mean velocity in the transversal section of the fluid,  $Q$  is the flow rate,  $f$  is the resistance factor (friction factor),  $h_\ell$  is the head loss,  $D$  is the diameter of the tube,  $L$  is its length,  $\rho$  is the density of the liquid and  $g$  is the acceleration of gravity.

To use Eqs. (7a, b) in differential form, and applied to eddy movements, an ideal scheme was conceived, consisting of a stationary isotropic turbulence field with eddies encompassing the range of sizes from the energy containing scale (large eddies) to the so-

called dissipation scale (small eddies). Instantaneous velocity profiles from flows in opposite directions are ideally sketched in Fig. 1a, showing different characteristic mean  $V$  values (scales) for different  $\ell$  length scales (as in Richardson's poem "big whorls have little whorls...", quoted by [Nature Physics, 2016](#)) and related to momentary flow rates advancing through the cross-section  $A$  of the shown differential tube length  $dL$ .

The characteristic velocity of turbulence is the RMS velocity, varying with  $\mathcal{V}$ , being thus  $V$  a measure of it, and stationarity implies mean variables constant in time. For the differential tube length  $dL$  of Fig. 1c, Eqs. (7a, b) produce:

$$dh_\ell = f \frac{dL V^2}{\ell 2g} \tag{8a}$$

$$d\dot{E} = gVA dh_\ell \tag{8b}$$

Two simplifying hypotheses were applied sequentially in the present step: i)  $\ell$  is taken as a constant for the "tube" length  $dL$ , and ii)  $d\mathcal{V}=AdL$ . It results, after integration:

$$\dot{E} = \varepsilon \mathcal{V} = \frac{1}{2\ell} \int_{\mathcal{V}} fV^3 d\mathcal{V} \tag{9}$$

For isotropy,  $\ell$  may be related to the volume of the eddy through  $\ell = (6\mathcal{V}/\pi)^{1/3}$ :

$$\varepsilon \mathcal{V}^{4/3} = \left(\frac{\pi}{6}\right)^{1/3} \frac{1}{2} \int_{\mathcal{V}} fV^3 d\mathcal{V} \tag{10}$$

Equation (10) involves two parameters of Eq. (6). Differentiating the logarithm of Eq. (10) and multiplying the result by  $\varepsilon \mathcal{V}$  leads to:

$$\frac{4\varepsilon}{3} d\mathcal{V} + \mathcal{V} d\varepsilon = \dot{E} d\ln \left[ \int_{\mathcal{V}} fV^3 d\mathcal{V} \right] \tag{11}$$

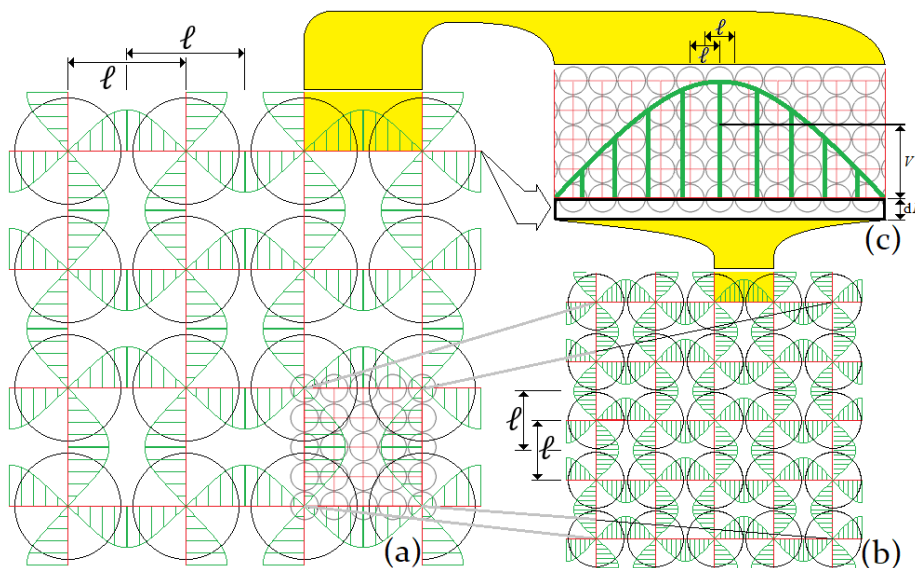


**Fig. 1. Ideal turbulence field showing a) the multicuity of length scales, b) the ideal distribution of eddies showing opposite movements in which the boundaries between them define the infinitesimal tube length; c) the tube length  $dL$  where the Darcy-Weisbach equation is applied.**

The second member was defined as  $d\psi$ , resulting:

$$\frac{4\varepsilon}{3} d\mathcal{V} + \mathcal{V}d\varepsilon = d\psi \tag{12a}$$

$$d\psi = \dot{E} d\ln\left(\int_{\mathcal{V}} fV^3 d\mathcal{V}\right) \tag{12b}$$

Equations (12a, b) furnish valuable empirical facts to Eq. (6). From the parcels of Eqs. (6) and (12a) we have  $\alpha=4/3$ ,  $\beta=\delta$ , and  $d\phi=x^\beta d\psi$ , thus:

$$d\phi = \frac{4x^\beta}{3} \varepsilon d\mathcal{V} + x^\beta \mathcal{V}d\varepsilon \tag{13a}$$

$$d\phi = x^\beta \dot{E} d\ln\left(\int_{\mathcal{V}} fV^3 d\mathcal{V}\right) \tag{13b}$$

For the remaining unknown exponent  $\beta$  the formulation was solved for  $x$ , and experimental results of turbulent transport were used. The Schwarz equality between the second derivatives of interchanged variables was used in Eq. (13a) in the form:

$$\frac{d}{d\varepsilon}\left(\frac{d\phi}{d\mathcal{V}}\right)\Big|_{\mathcal{V}} = \frac{d}{d\mathcal{V}}\left(\frac{d\phi}{d\varepsilon}\right)\Big|_{\varepsilon} \tag{14}$$

The derivatives are taken in relation to one variable while the second variable remains constant. In Eq. (14) the derivatives of  $\phi$  were taken in relation to the differentials of Eq. (13a), implying that  $x$  may be a function of  $\varepsilon$ , or  $\mathcal{V}$ , or “ $\varepsilon$  and  $\mathcal{V}$ ” together. The different possibilities were tested, and the dependence  $x=x(\varepsilon)$  showed to be more adequate (by trial-and-error). The result for Eqs. (13a) and (14) is:

$$\frac{dx}{x} = -\frac{1}{4\beta} \frac{d\varepsilon}{\varepsilon} \tag{15}$$

$$x = \theta_1 \varepsilon^{-\frac{1}{4\beta}} \tag{16}$$

$x$  is thus a power law of  $\varepsilon$ .  $\theta_1$  is the integration constant that adjusts the dimensions of both members of Eq. (16). This power law is an empirical evidence already described in the literature by different authors along the time. For example, using the pre-sent notation, [Calderbank and Moo-Young \(1961\)](#) expressed heat and mass transfer coefficients from solid surfaces to turbulent fluids as  $x \propto (\varepsilon\nu)^{1/4}$ , being  $\nu$  the kinematic viscosity. [Lamont and Scott \(1970\)](#) added more information of the compounds into contact through the Schmidt number  $Sc$ , suggesting  $x \propto Sc^{1/2}(\varepsilon\nu)^{1/4}$ . [Chu and Jirka \(2003\)](#) worked with oxygen absorption by water in channels subjected to wind, confirming  $x \propto \varepsilon^{1/4}$ . [Chen \(2019\)](#) worked with impeller agitators and bubbles, adding the diameter of the bubbles and the volume fraction of the gaseous phase in the equation for  $x$  confirming also the dependence  $x \propto \varepsilon^{1/4}$ . Results of own experiments were presented by [Schulz \(1991\)](#) and [Schulz and Giorgetti \(1991\)](#) for the dissolution of solids of oxalic acid floating at the water surface in

two experimental devices: i) a 0.10 m<sup>3</sup> baffled water tank agitated by an impeller which rotation varied from 0 to 250 rpm; and ii) a 22.0 m length flume in which a smooth bed and five different sand and gravel bed roughnesses were tested: 0.97 mm, 2.38 mm, 4.76 mm, 6.35 mm, and 9.51 mm, and imposing flow rates varying in the range from 16.91 l/s to 29.13 l/s. The dissolution results are shown in Fig. 2, and the best adjustment for  $x$  is given by Eq. (17).

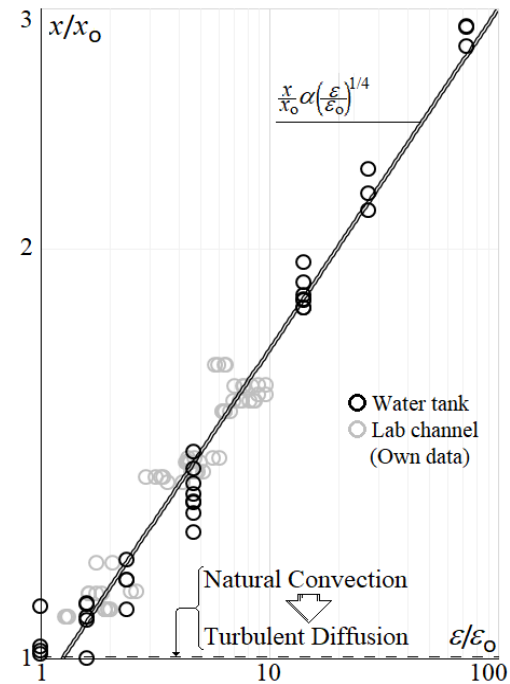


**Fig. 2. Oxalic acid mass transfer coefficient against power dissipations.  $\varepsilon_0$  and  $x_0$  define the transition from natural convection to turbulent diffusion.**

$$x = \left[1.496 \cdot 10^4 e^{-\left(\frac{6444}{T}\right)}\right] \varepsilon^{\frac{1}{4}} \tag{17}$$

For the presented coefficients the dimension of  $x$  is m/s, and the dimension of  $\varepsilon$  is m<sup>2</sup>/s<sup>3</sup>. The dissolution of oxalic acid in water is a function of the temperature  $T$  (expressed in Kelvin), and of turbulence according the  $\varepsilon^{1/4}$  power law. Experiments thus point to  $\beta = -1$  in Eq. (16), so that Eqs. (13a, b) assume the forms:

$$d\phi = \frac{4}{3x} \varepsilon d\mathcal{V} + \frac{\mathcal{V}}{x} d\varepsilon \tag{18a}$$

$$d\phi = \frac{\dot{E}}{x} d\ln\left(\int_{\mathcal{V}} fV^3 d\mathcal{V}\right) \tag{18b}$$

Equations (18a, b) aggregate consolidated empirical results that can be traced back by performing the inverse calculations ([Schulz 2001](#)). As interesting result, it is analogue to the Thermodynamics formulation of thermal radiation, as evidenced in Table 1.

**Table 1 Analogy between turbulence and thermal radiation formulations**

Turbulence	Thermal Radiation
$d\phi = \frac{4}{3x} \varepsilon d\mathcal{V} + \frac{\mathcal{V}}{x} d\varepsilon$	$dS = \frac{4}{3T} u d\mathcal{V} + \frac{\mathcal{V}}{T} du$
$\varepsilon = \theta_2 x^4$	$u = \theta_3 T^4$
$d\phi = \frac{d\psi}{x}$	$dS = \frac{d\bar{Q}}{T}$
$\psi$	$\bar{Q}$
$\phi$	$S$
$x$	$T$
$\varepsilon$	$u$
$\mathcal{V}$	$\mathcal{V}$

The analogy is meant for the form of both formulations, and not for the meaning of the variables. In Table 1  $S$  is the entropy,  $T$  is the absolute temperature,  $u$  is the energy density,  $\bar{Q}$  is the heat,  $\theta_2 = \theta_1^{-1/4}$ , and  $\theta_3$  is the integration constant of the thermal radiation fourth power law. The radiation formulation is usually related to the black body, an ideal condition in radiation studies, while the turbulence formulation represents the isotropic case, also an ideal condition in turbulence studies.  $d\phi$  is defined by Eq. (18b), which relates it to parameters with known physical meaning. A further interesting aspect is that the interaction between turbulent movements in opposite directions (ideal condition of Fig. 1) involves a friction factor, a parameter known to be linked to the Reynolds number (also adopted here) and to a ‘relative roughness’, which still needs further complementary studies.

### 3. SPECTRAL VARIATIONS

The study of the black body radiation led to the study of the radiation spectrum in Thermodynamics (see for example [Osada 1972](#); [Stewart and Johnson, 2016](#)). The similarity between the formulations of Table 1 suggests also to search for spectral functions in turbulence. Equations (18a, b) lead to:

$$\frac{4}{3} \frac{d\mathcal{V}}{\mathcal{V}} + \frac{d\varepsilon}{\varepsilon} = d \ln \left( \int_{\mathcal{V}} f V^3 d\mathcal{V} \right) \quad (19)$$

Integrating the logarithms and then applying the derivative in relation to  $\mathcal{V}$  results in:

$$\frac{4}{3} \mathcal{V}^{1/3} \varepsilon + \mathcal{V}^{4/3} \frac{d\varepsilon}{d\mathcal{V}} = \theta_4 f V^3 \quad (20)$$

$\theta_4$  is an integration constant. A generic volume  $\mathcal{V}(k)$  between the smallest and the largest eddy is related to a generic velocity  $V(k)$ , and to a generic power loss  $\varepsilon(k)$ . Eq. (1) relates this  $V(k)$  to the energy spectrum  $E(k)$  using a free limit of integration as:

$$\frac{3}{2} V^2 = \int_k E(k) dk \quad (21)$$

This defines the variation of  $V$  with  $k$ . From Eq. (2) the volume of an eddy is  $\mathcal{V} = (\pi/6)/k^3$ . Coupling Eqs.

(20) and (21), dividing by  $\frac{4}{3} \mathcal{V}^{1/3}$ , and rearranging leads to:

$$\begin{aligned} & \frac{-k}{4} \frac{d\varepsilon(k)}{dk} + \varepsilon(k) - \\ & - \frac{3}{4} \left( \frac{6}{\pi} \right)^{1/3} \theta_4 f k \left( \frac{2}{3} \int_k E(k) dk \right)^{3/2} = 0 \end{aligned} \quad (22)$$

Equation (22) was used to verify possible forms of the spectra  $\varepsilon(k)$  and  $E(k)$ .

#### 3.1 Spectra for $f$ Containing Viscosity: Euler Governing Equation

In principle, if effects of viscosity are relevant, at least one coefficient in Eq. (22) must be related to it, a condition satisfied by  $f$ . Adequate forms of  $f$  must be applied to consider viscosity. From the empirical knowledge on pipe flows,  $f$  depends on viscosity through the Reynolds number of the pipe,  $Re_D$ , adapted here to the eddy Reynolds number,  $Re_k = V/k \nu$  or  $Re_\ell = V\ell/\nu$ . For low Reynolds numbers the result  $f = 64/Re_k$ , was used as the best choice in the absence of other references, resulting in

$$\begin{aligned} & \frac{-1}{4k} \frac{d\varepsilon(k)}{dk} \\ & + \frac{\varepsilon(k)}{k^2} - 32 \left( \frac{6}{\pi} \right)^{1/3} \theta_4 \nu \int_k E(k) dk = 0 \end{aligned} \quad (23)$$

The power dissipation  $\varepsilon$  depends on  $k$ . Both variables are already linked in the traditional spectral analyses of isotropic turbulence, Eq. (3), used here with a free limit of integration:

$$\varepsilon(k) = 2\nu \int_k k^2 E(k) dk \quad (24)$$

A form of the energy spectrum is obtained from the derivative of Eq. (24):

$$E(k) = \frac{1}{2\nu k^2} \frac{d\varepsilon(k)}{dk} \quad (25)$$

Using Eq. (25) into Eq. (23), taking the derivative in relation to  $k$ , and rearranging leads to the differential governing equation for  $\varepsilon$  given by the present formulation:

$$k^2 \frac{d^2 \varepsilon(k)}{dk^2} - IJ k \frac{d\varepsilon(k)}{dk} + 8\varepsilon(k) = 0 \quad (26)$$

Equation (26) is a Euler differential equation with one unknown coefficient,  $IJ = 5-64\theta_4(6/\pi)^{1/3}$ , which carries the integration constant  $\theta_4$ . The quantification of the power dissipation in turbulent flows is still a matter of discussion ([Hoque et al. 2015](#), [Wang et al. 2021](#)), being related to the entropy generation rate ([Bejan 1982](#)). In this sense, Eq. (26) for the spectrum  $\varepsilon(k)$  is a new information that may help this quantification. The solution of Eq. (26) depends on the two values of  $r$  of the basic substitution  $\varepsilon = k^r$  (e.g., [Boyce and DiPrima 2009](#)), given by:

$$r_1 = \frac{IJ + 1}{2} + \sqrt{\left[\frac{IJ + 1}{2}\right]^2 - 8} \quad (27a)$$

$$r_2 = \frac{IJ + 1}{2} - \sqrt{\left[\frac{IJ + 1}{2}\right]^2 - 8} \quad (27b)$$

If  $r_1 \neq r_2$  and both are Real numbers, the solution is:

$$\varepsilon(k) = C_1 k^{r_1} + C_2 k^{r_2} \quad (28)$$

$$\text{and } E(k) = T_1 k^{r_1-3} + T_2 k^{r_2-3} \quad (29)$$

$C_1, C_2, T_1,$  and  $T_2$  are integration constants that adjust the dimensions of the equations. The solutions of  $\varepsilon(k)$  are power laws of  $k$ , and, from Eq. (25), power laws also apply to the energy spectrum  $E(k)$ . The theoretical result of governing Eq. (26) confirms experimental results that present power law spectra with several different exponents (for example [Voitenko and De Keyser, 2011](#); [Xia et al., 2013](#); [Alexandrova et al. 2013](#), [Goldstein et al. 2015](#), [Verscharen et al. 2021](#)). Also generic exponents are shown in some studies, like the exponent ‘ $-\alpha$ ’ that follows the  $-5/3$  spectrum in [Bourouaine et al. \(2012\)](#). For boundary conditions that lead to  $IJ=19/3 \approx -6.33$ , Eqs. (27a, b) produce  $r_1=4/3$  and  $r_2=6.0$ , and the energy spectrum of Eq. (29) has powers  $-5/3$  and  $3.0$ . That is, the known exponent  $-5/3$  of the Kolmogoroff /Obukhoff/Onsager’s spectrum is obtained for situations in which  $f$  is proportional to the viscosity and with power dissipation occurring in the whole range of wavenumbers. The existence of the  $-5/3$  power for nonequilibrium situations (different of the Kolmogoroff proposal) was already shown and discussed for example by [Vassilicos \(2015\)](#), and the present formulation indicates that this result is in fact possible. Equations (28) and (29) also show that cut-off wavenumbers may limit the evolution of  $\varepsilon(k)$  and  $E(k)$ , depending on values and signs of  $r_{1,2}, C_{1,2}$ , and  $T_{1,2}$ . Figure 3 shows examples of  $-5/3$  spectra using various values of  $r_2$  to cut their evolutions. For continuous evolutions (no cutoff),  $T_1$  or  $T_2$  are set to zero.

Equations (27a, b) show that equal Real roots  $r_1=r_2=r$  occur for  $IJ = -1 \pm 2\sqrt{8}$ , being  $r$  either  $\sqrt{8}$  or  $-\sqrt{8}$ .  $\varepsilon(k)$  and  $E(k)$  are now given by Eqs. (30a, b) and (31a, b):

$$\varepsilon(k) = \mathcal{S}_A k^{\sqrt{8}} \left( \ln \frac{k}{k_R} \right) \quad (30a)$$

$$\text{and } E(k) = \mathcal{S}_B k^{\sqrt{8}-3} \left( \ln \frac{k}{k_R} \right) \quad (30b)$$

$$\varepsilon(k) = \mathcal{S}_C k^{-\sqrt{8}} \left( \ln \frac{k}{k_R} \right) \quad (31a)$$

$$\text{and } E(k) = \mathcal{S}_D k^{-\sqrt{8}-3} \left( \ln \frac{k}{k_R} \right) \quad (31b)$$

The integration constants  $\mathcal{S}_A, \mathcal{S}_B, \mathcal{S}_C, \mathcal{S}_D$ , may be positive or negative, which compose with the sign of the logarithm of  $k/k_R$ . The integration constant  $k_R$  has the physical meaning of a reference wavenumber. The logarithm in Eqs. (30a, b) and (31a, b) also

produce spectra with beginning or ending cutoff wavenumbers, and several values are exemplified in Figs. 4 a, b and 5 a,b, limiting the spectra at the left or at the right sides.

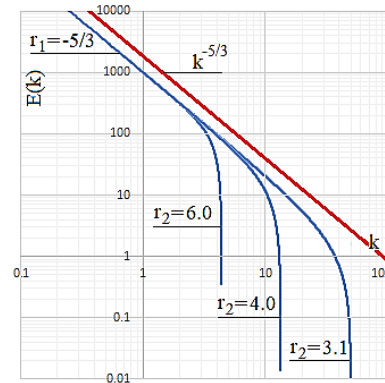


**Fig. 3. Equation (29) for different values of  $r_2$ , which adjusts the different observable cutoff wavenumbers.**

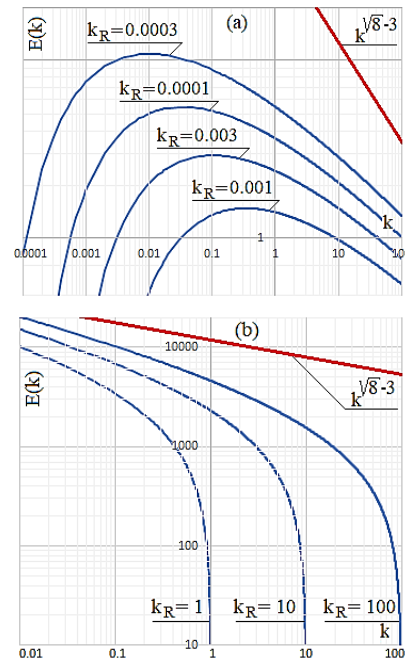


**Fig. 4. a) Left cutoff of the energy spectra using Eq. (30b); b) right cutoff using Eq. (30b).**

Spectra of  $E(k)$  with the  $\pm\sqrt{8}-3$  exponents of Eqs. (30b) and (31b) were juxtaposed with the  $-5/3$  spectrum of turbulence in Fig. 6. The  $\sqrt{8}-3$  exponent is better suited for the left side of the spectra, while the  $-\sqrt{8}-3$  exponent is better suited for the right side, the last being the dissipative range of the spectra. Figure 6 compares theoretical and literature experimental data evidencing the interesting pattern of this juxtaposition. Figure 6 does not present cutoff wavenumbers because of the limits of the measured values, but proper  $k_R$  values may be used in Eqs. (30b) and (31b). Juxtapositions with other power laws resulting from Eq. (29) are also possible.

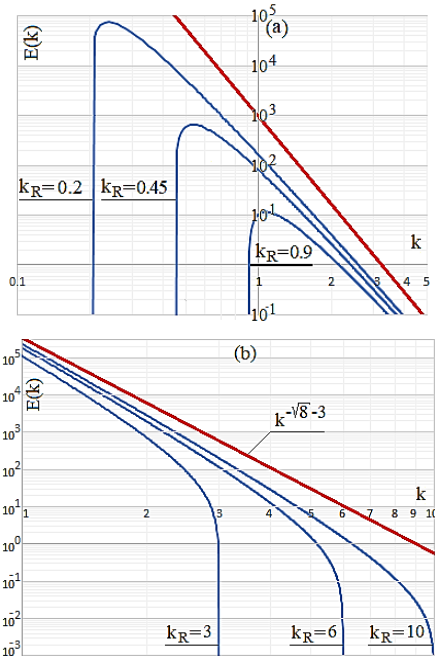


**Fig. 5. a) Left cutoff of the energy spectra using Eq. (31b); b) right cutoff using Eq. (31b).**

If  $r_1$  and  $r_2$  are conjugate complex numbers, they are represented as:

$$r_1 = \frac{IJ + 1}{2} + i \sqrt{\left[\frac{IJ + 1}{2}\right]^2 - 8} = \omega_1 + i\omega_2 \quad (32a)$$

$$r_2 = \frac{IJ + 1}{2} - i \sqrt{\left[\frac{IJ + 1}{2}\right]^2 - 8} = \omega_1 - i\omega_2 \quad (32b)$$

The solutions for  $\varepsilon$  and  $E(k)$  are then given by:

$$\varepsilon(k) = k^{\omega_1} \begin{bmatrix} C_1 \cos(\omega_2 \ln k) \\ + C_2 \sin(\omega_2 \ln k) \end{bmatrix} \quad (33a)$$

$$E(k) = k^{\omega_1 - 3} \frac{\begin{bmatrix} T_1 \cos(\omega_2 \ln k) \\ + T_2 \sin(\omega_2 \ln k) \end{bmatrix}}{\nu} \quad (33b)$$

In this case the spectra have, in principle, a periodic character along the wavenumber axis. However, fluids dissipate energy through its viscous property and have  $E(k)$  evidently limited by viscosity in the smaller scales. Further, for fluids occupying finite regions, eventual larger movements (larger eddies) are also limited by the dimensions of these regions. Having attained zero mean kinetic energy on both length extremes, turbulent fluids do not “recover” movements at smaller or larger wavenumbers (no periodicity).

Equations (33a, b) also furnish bounded turbulent energy spectra, but with two limiting extremes. The start and end points are given by the sine and cosine functions. The general slope of the curve (or succession of curves) and its position in the graph is governed by  $\omega_1$ ,  $\omega_2$ ,  $T_1$  and  $T_2$ . Figure 7 illustrates an energy spectrum of Eq. (33b).

A further analysis of Eqs. (27a, b) considers the value of  $IJ$  representing boundary conditions of specific problems (physical impositions). Figure 8 shows the evolution of the exponents  $r_{1-3}$  and  $r_{2-3}$  as function of  $IJ$  in the interval  $(-\infty, \infty)$ , and Table 2 shows the limiting values of  $-3$  (central asymptote of Fig. 8),  $-3 + \sqrt{8}$ ,  $-3 - \sqrt{8}$  (with  $\sqrt{8} = 2\sqrt{2}$ ). The classical value of  $-5/3$  is also evidenced in the table. The  $45^\circ$  angle between the two asymptotes of Eqs. (27a, b) produces projections between the two sets of axes with the factor  $\cos(45^\circ) = \sqrt{2}$ . Figure 8 shows  $r_{1-3}$  and  $r_{2-3}$  values of intersection points of the axes of the function that coincide with some classical exponents,

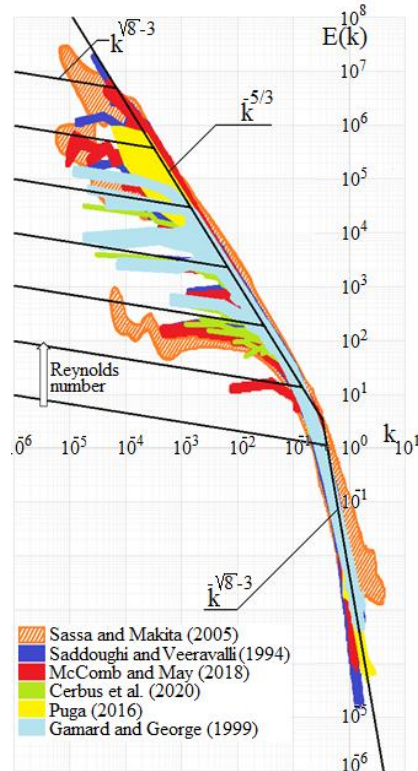


**Fig. 6. Good superposition between literature data and theoretical trends of  $E(k)$  as proportional to  $k^{-5/3}$  and to  $k^{\pm 5/8-3}$ , the last obtained by solving Eq. (26) for equal real roots.**

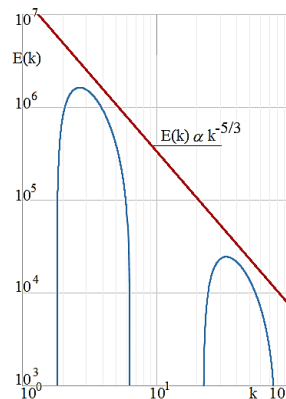


**Fig. 7. Example of  $E(k)$  for conjugate complex roots of Eqs. (27a, b). Periodicity is not expected for space-restricted and viscous-dissipative fluid flows.**



**Table 2: Power law exponents as functions of  $IJ$**

$IJ$	$r_1$	$r_2$	$r_1-3$	$r_2-3$
$\rightarrow-\infty$	$\rightarrow 0$	$\rightarrow-\infty$	$\rightarrow-3$	$\rightarrow-\infty$
-100	-0.08087	-98.919	-3.0809	-101.92
-50	-0.16381	-48.836	-3.1638	-51.836
-30	-0.27854	-28.722	-3.2785	-31.722
-20	-0.43082	-18.569	-3.4308	-21.569
-10	-1	-8	-4	-11
-7.8	-1.5132	-5.2868	-4.5132	-8.2868
-7.6	-1.6	-5	-4.6	-8
-7	-2	-4	-5	-7
-6.7	-2.5	-3.2	-5.5	-6.2
$-1-2\sqrt{8}$	$-\sqrt{8}$	$-\sqrt{8}$	$-3-\sqrt{8}$	$-3-\sqrt{8}$
	$\updownarrow$	Complex solutions	$\updownarrow$	
$-1+2\sqrt{8}$	$\sqrt{8}$	$\sqrt{8}$	$-3+\sqrt{8}$	$-3+\sqrt{8}$
4.6569	2.8398	2.8171	-0.16017	-0.18293
5	4	2	1	-1
5.6	5	1.6	2	-1.4
6	5.5616	1.4384	2.5616	-1.5616
19/3	6	4/3	3	-5/3
8	8	1	5	-2
10	10.217	0.78301	7.2170	-2.2170
20	20.612	0.38813	17.612	-2.6119
30	30.740	0.26025	27.740	-2.7398
50	50.842	0.15734	47.843	-2.8427
100	100.92	0.07927	97.921	-2.9207
$\rightarrow\infty$	$\rightarrow\infty$	$\rightarrow 0$	$\rightarrow\infty$	$\rightarrow-3$

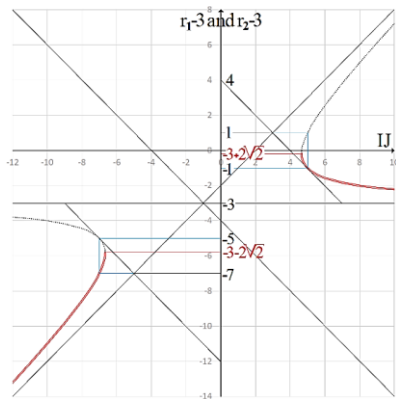


**Fig. 8. Exponents  $r_1-3$  and  $r_2-3$  against  $IJ$ . The asymptote  $r_1-3=r_2-3=-3$  is the central horizontal line. Classical exponents are shown in the vertical axis together with the  $-3\pm\sqrt{8}$  results.**

like 4 (Batchelor quoted by Heisenberg 1948), and 7 (Heisenberg 1948). This geometrical characteristic may be used as a mnemonical tool for the mentioned literature exponents, and to evidence the limiting values of of  $-3$ ,  $-3+\sqrt{8}$ , and  $-3-\sqrt{8}$ . The exponent  $-3$  is commonly found in experimental studies (Tung 2003; Brannigam et al. 2015, for example). Figure 9 shows data of very different experiments plotted together. The axes were normalized for the origin to coincide with the intersection point of the spectra slope lines  $-5/3$  and  $-3$ . Results for solar wind spectra are generally presented following slopes around  $-\sqrt{8}\sim -2.82$ . The data of the ocean boundary layer are for concurrent velocities (Lien and Sanford 2001).

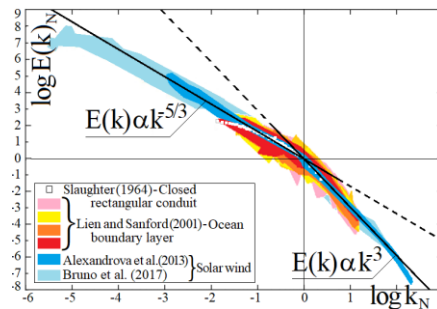


**Fig. 9, Results of spectra slopes tending to  $-3$ . Good superposition between data and theory.**

**3.2 Spectra for  $f$  Without Viscosity:  $5/3$  Law**

Certainly, the most used energy spectrum in turbulence studies is the Kolmogoroff/Obukhoff/Onsager spectrum, obtained for the inertial subrange, an ideal region along the wavenumbers where viscosity is not relevant and  $\varepsilon$  is taken as a constant parameter, also used for the scaling of length and velocity in the highest limiting wavenumber. In an earlier stage of the studies in turbulence, the energy transfer, or energy cascade was explained to occur from the larger to the smaller eddies, the firsts containing or storing the turbulent kinetic energy, and the lasts acting as a drain that consumes or dissipates this energy. In this sense, smaller eddies are generated by larger eddies and energy is transferred to them until the dissipation scale. This unidirectional point of view was then changed to the possibility of having also the energy cascade occurring from smaller to larger eddies. In this sense, by adding turbulent kinetic energy in the region of small eddies, they compose to generate

larger eddies, so that in fact energy is transferred to the larger movement scales. A simple example is a jar of water to which concentrated fruit juice is added and a thin wire or wood stick is used to agitate the mixture with short movements. Despite the small-scale turbulent movements generated around the stick, they compose and generate larger scale movements that attain the scale of the jar itself and help the whole mixture. A net “inverse” energy transfer occurs, being also dissipated in the larger scales. An extensive review of direct and inverse cascades may be found in [Alexakis and Biferale \(2018\)](#), and measurements of a specific study may be found in [Neely \(2013\)](#), for example.

Although not necessary to obtain the  $-5/3$  power (as already shown), the present formulation also leads to this law when using Kolmogoroff’s hypotheses (together with the studies of [Obukhoff 1941](#) and [Onsager 1945](#)). Both energy cascades (direct and inverse) may occur simultaneously. Figures 10 a, b, c show sketches of several cases, with the energy input concentrated at a chosen wavenumber region, being then distributed to larger and smaller scales produced by the specific agitation conditions. Power dissipates in the whole wavenumber range, and a constant distributed  $\varepsilon(k)$  was used to fit Kolmogoroff/Obukhov/Onsager’s condition (constant energy flows from the largest to the smallest eddies, being dissipated there). Figure 9 also shows regions where dissipation is eventually more condensed, indicated as “final energy drains”.

In Eq. (22), following the analogy with flows in pipes and the knowledge of the behaviour of the friction factor,  $f$  assumes a constant value for higher Reynolds numbers. The spectra may evolve between the limits  $k_E$  and  $k_D$  (Figs. 10a and b), or between the limits  $k_E$  and  $k_\ell$ , (left side of Fig. 10c) and  $k_\ell$  and  $k_D$ , (right side of Fig. 10c). Constant  $\varepsilon(k)=\varepsilon$  implies that  $d\varepsilon/dk=0$ , so that Eq. (22) furnishes:

$$\text{Coefficient} \cdot \left(\frac{\varepsilon}{k}\right)^{\frac{2}{3}} = \int_k E(k) dk \quad (34)$$

The derivative of Eq. (34) leads to:

$$E(k) = \mathcal{A} \varepsilon^{\frac{2}{3}} k^{-\frac{5}{3}} \quad (35)$$

The coefficient  $\mathcal{A}$  involves the integration constant  $\theta_4$  and the adequate sign. Equation (35) is the Kolmogoroff/Obukhoff/Onsager spectrum obtained from the present formulation when using Kolmogoroff’s hypotheses. Empirical studies suggest for  $\mathcal{A}$  a value of about 1.5 (see, for example, [Pope 2000](#) and [Cheng et al. 2010](#)).

Because the power dissipated at the left side (bass range in Fig. 11a) may be different from that dissipated at the right side (crescendo range in Fig. 11b), the vertical position of the spectral function may also be different at both sides. The multiplicative factor  $\varepsilon^{2/3}$  in Eq. (35) dislocates vertically the function in the log/log graph as shown in Fig. 11.

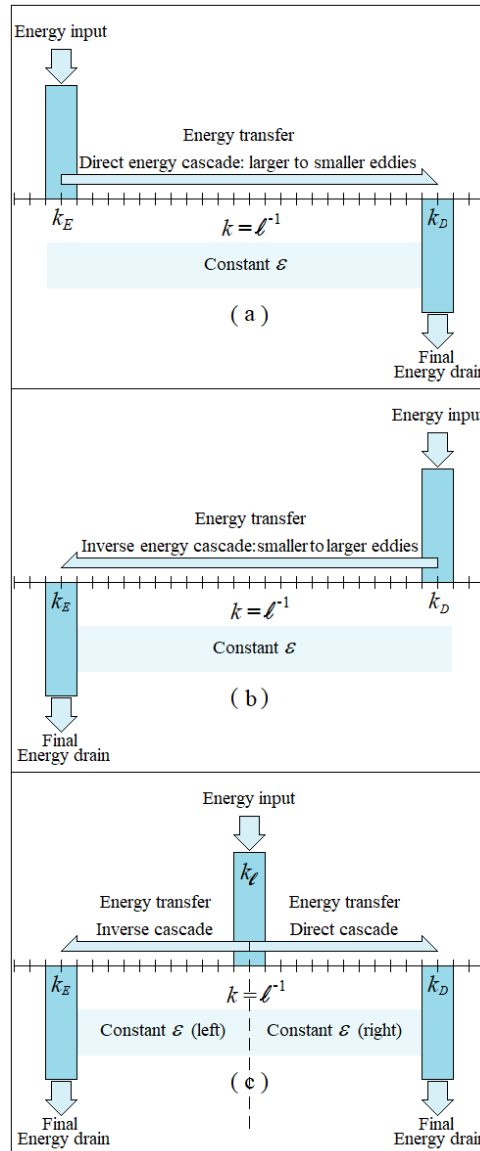


**Fig. 10. Kolmogoroff’s hypotheses usually adopted for the energy spectrum; a) Direct energy cas-cade in the Kolmogoroff sense; b) Inverse energy cascade; c) Concomitant direct/inverse cascades.**

#### 4. CHARACTERISTIC PARAMETERS

##### 4.1 Characteristic Power Dissipation

The present formulation involves a friction factor for opposite turbulent motions (Fig. 1), inherited from the Darcy-Weisbach equation, which allows observing the effect of length scales through the eddy’s Reynolds number ( $Re_k=V/k\nu$ , or  $Re_\ell=V\ell/\nu$ ). Known semi-empirical results for turbulence scales may also be obtained from Eqs. (18a, b), equated here to obtain Eq. (36), resembling Eqs. (12a, b).

$$\frac{4\varepsilon}{3} d\nu + \nu d\varepsilon = \dot{E} d\ln \left( \int_\nu fV^3 d\nu \right) \quad (36)$$

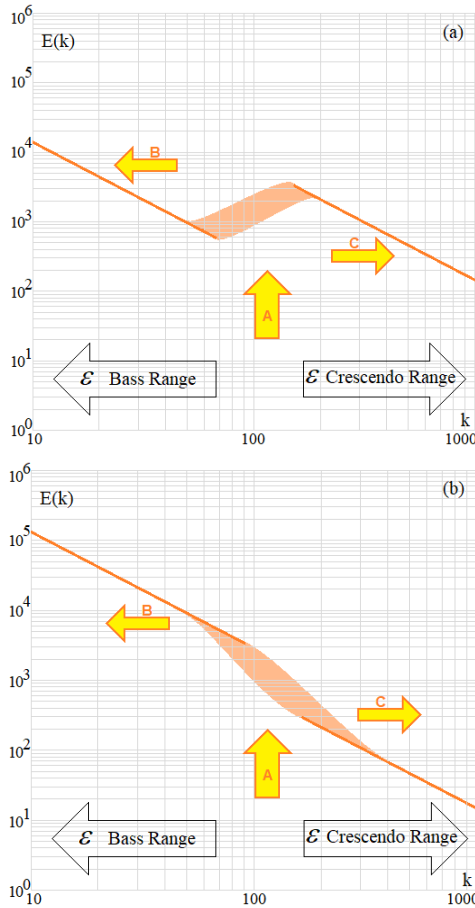


**Fig. 11: Dislocated spectra for distinct characteristic  $\varepsilon$  at distinct regions of the wavenumber axis; A=apport of energy; B= bass range dissipation (low  $k$ ); C= crescendo range dissipation (high  $k$ ); a) lower  $\varepsilon$  in bass range; b) higher  $\varepsilon$  in bass range.**

Taking a mean constant velocity  $V$  for the volume, dividing Eq. (36) by  $\dot{E}$  and presenting the result in the form of differentials of logarithms leads to:

$$\frac{4}{3} d\ln(V) + d\ln(\varepsilon) = d\ln\left(V^3 \int_V f dV\right) \quad (37)$$

The integration of Eq. (37) produces, for the characteristic dissipation  $\varepsilon$ :

$$\varepsilon = \frac{\Xi V^3 \int_V f dV}{\nu^{4/3}} \quad (38)$$

$\Xi$  is an integration constant. Two different cases are considered: i) high agitation (large eddy Reynolds numbers, constant  $f$ ); ii) low agitation (small eddy Reynolds numbers,  $f=64\nu/(V\ell)$ ). Using  $\ell=(6\nu/\pi)^{1/3}$  for both cases, the integration of Eq. (38) furnishes for the characteristic  $\varepsilon$ , respectively:

$$\varepsilon = G_1 \frac{V^3}{\ell} \quad (39a)$$

$$\text{and} \quad \varepsilon = G_2 \left(\frac{\sqrt{\nu} V}{\ell}\right)^2 \quad (39b)$$

$G_1$  and  $G_2$  are constants. Equations (39a, b) are usual in turbulence studies (see Hinze, 1959). In the present study they are linked to the friction factor, which expresses the interaction between eddies (Fig. 1).

#### 4.2 Mean Velocity Scales

Equation (40a) defines the isotropic turbulence kinetic energy ( $KE$ ), which, used for an eddy of generic scale  $\ell$  together with Eqs. (39a, b) leads, respectively, to Eqs. (40b) and (40c):

$$KE = \frac{V^2}{2} + \frac{V^2}{2} + \frac{V^2}{2} = \frac{3V^2}{2} \quad (40a)$$

$$KE = \frac{3}{2G_1^{2/3}} (\varepsilon\ell)^{2/3} \quad (40b)$$

$$\text{and} \quad KE = \frac{3}{2G_2} \frac{\varepsilon\ell^2}{\nu} \quad (40c)$$

Again, Eqs. (40 b, c) are known in the literature of turbulence (Hinze, 1959). Equations (39b) and (40c) are valid for low  $Re_k$  eddies (low  $V$  and/or  $\ell$ , high  $\nu$ ), and Eqs. (39a) and (40b) are valid for high  $Re_k$  eddies (high  $V$  and/or  $\ell$ , low  $\nu$ ). The conclusions obtained from the friction factor related to the interaction between turbulent movements (Fig. 1) give support to the usual approximations adopted in the literature.

Because the  $-5/3$  spectrum was obtained for  $f$  with and without  $\nu$ , Eqs. (39a, b) may equally describe turbulence parameters for a range of eddy sizes (wavenumbers). By equating them, a constant Reynolds number is obtained ( $G_3$  is a constant):

$$\frac{V\ell}{\nu} = G_3 \quad (41a)$$

Further, Eqs. (39a) and (41a) produce (41b):

$$V = G_4 (\nu\varepsilon)^{1/4} \quad (41b)$$

$G_4$  is a constant coefficient.

#### 4.3 Mean Length Scales

Equations (39b) and (41a) produce (41c):

$$\ell = G_5 \frac{\nu^{3/4}}{\varepsilon^{1/4}} \quad (41c)$$

$G_5$  is a constant coefficient. Equations (41b, c) are the Kolmogoroff velocity and length scales, considered valid for the smaller eddies, with  $G_3$  usually equal to 1.0.  $f=64/Re_\ell$  and  $f=\text{constant}$  thus resulted in consistent equations for the characteristic  $\varepsilon$ .

#### 4.4 Velocity and Length Scales Merged with the Characteristic Power Dissipation

An equivalent form of Eq. (39b) is obtained by adopting  $f \propto Re_\ell^{-p}$  (laminar case, and turbulent case for smooth pipes as shown by Holland and Bragg, 1995, who mention the equation of Blasius and the equation of Drew), and results in

$$\varepsilon = G_6 \left(\frac{V^3}{\ell}\right) \frac{1}{Re_\ell^p} \quad (42)$$

$G_6$  is a constant coefficient. Equations (39a) and (42) produce Eq. (41a) for any  $p$ . Further, Eqs. (41a) and (42) produce:

$$\varepsilon = G_7 \left( \frac{V^{3-p} \mathcal{V}^p}{\rho^{1+p}} \right) \quad (43)$$

Equation (43) suggests that the characteristic  $\varepsilon$  is not uniquely defined along the spectrum. Additionally, it leads to the usual expressions of the literature for big and small  $\ell$  (or  $k$ ) scales.  $p = 0$  is used for no influence of viscosity, and  $p = 1$  for the 1<sup>st</sup> power influence. New values  $p$  and functions  $f$  may be tested in similar studies. Flows in tubes show that the friction factor has a complex behaviour with the Reynolds number, and involves additional multiscale geometrical characteristics in its quantification (tube diameter, roughness). General turbulent flows also present complex behaviours and are influenced by different scales, inducing the continuity of studies involving  $f$ , and that combine consolidated empirical knowledge of different sources of applied fluid mechanics.

## 5. FINAL REMARKS AND CONCLUSION

In this study empirical and semi-empirical independent results of turbulence were joined in an alternative formulation using the consolidated knowledge to grasp the behavior of turbulence variables in cases not considered in the original independent studies.

The Darcy-Weisbach equation for head losses and the power law for transfer coefficients formed the initial dyad of empirical equations. It allowed defining two auxiliary functions in differential form,  $d\phi$  and  $d\psi$ , and to link them to the power dissipation per unit mass  $\varepsilon$ , the volume of an eddy  $\mathcal{V}$ , the velocity scale of turbulence  $V$ , and the turbulent transfer coefficient  $x$ , using a thermodynamic-like equation that resembles the equation of the black body radiation.

The present study is a second option for the dimensionally obtained power law for isotropic turbulence (sequential studies of Kolmogoroff, Obukhoff and Onsager). Like [Onsager \(1945\)](#), four variables were used, one of which ( $\phi$ ) has its differential form ( $d\phi$ ) defined through the other three. [Onsager \(1945\)](#) used directly the energy spectrum. However, the parameter  $\phi$  used here is unknown *a priori*, and depends on the physical property transferred through turbulence, so that dimensional analyses are not promptly possible. About the turbulence transfer, instead of firstly inserting the viscosity as a relevant parameter in a dimensional analysis, and then discarding it when suggesting a power law, in the present study the *turbulent* transfer was introduced through the parameter  $x$  (remembering that viscosity relates to laminar momentum transfer). The formulation started from the definition of the power dissipation in differential form. Coefficients and exponents of the initial equation were obtained from empirical consolidated results.

This formulation allows treating power dissipation from a new point of view. Applying definitions from the theory of isotropic turbulence, a second order governing equation was obtained for the power dissipation per unit mass (Eq. 26) in the form of a Euler equation. It allows obtaining power spectra for the energy dissipation rate and for the turbulence kinetic energy as dependent on the wavenumber. There are no *a priori* limits for the values of the exponents of the spectra, which agrees with the broad range of exponents found in the literature. As expected, specific boundary conditions may lead to specific exponents. The -5/3 power law is obtained imposing the Kolmogoroff's conditions (equilibrium conditions) with constant power dissipation along the energy spectrum. Additionally, it was also shown that the -5/3 exponent may be attained for boundary conditions that do not follow the equilibrium condition, once more agreeing with the literature. The exponent -3, a result found in experiments performed in different turbulence studies described in the literature (oceans, channels, solar wind) is obtained as a limiting condition of the present formulation, increasing its potential of application.

The friction factor showed to be a useful parameter for the study of the characteristic energy and related mean turbulence scales. It allows considering different eddy's Reynold number  $Re_k$  or  $Re_\ell$  through a consolidated factor. The cases  $f=64/Re_k$  and  $f=constant$  were applied, resulting in consistent equations for the characteristic power dissipation  $\varepsilon$ , reproducing relations already existing in the literature. The testing of different forms of  $f$  in the context of turbulent interactions is still open to study.

The structure given to the formulation allows exploring possible extensions to bring together more empirical results. Power laws, spectral descriptions, the interpretation and use of the friction factor, are some of the usual concepts that were discussed here from a new point of view while testing this formulation. It is expected that this approach can be further im-proved, simplifying the understanding of turbulence phenomena and the interconnection between the concepts that we build for them.

## ACKNOWLEDGEMENTS

The author thanks Prof. Ingo Schulz for relevant initial advices and the financial support T. I. M *bó* 04031-928-2005 obtained through his person; and to Prof. Janka Neuwiem for decisive advices in the final part, and the financial support: K. I. E.*lce* 20061-936-2021.obtained through her person.

## REFERENCES

- Alexakis, A. and L. Biferale (2018). Cascades and transitions in turbulent flows, *Physics Reports* (767-769), 1-101.
- Alexandrova, O., C. H. K. Chen, L. Sorriso-Valvo, T. S. Horbury and S. D. Bale (2013). Solar wind turbulence and the role of ion instabilities, *Space Science Reviews* 178, 101-139.

- Badillo, A and O. K. Matar (2017). On the missing link between pressure drop, viscous dissipation, and the turbulent energy spectrum, *APS/123-QED*.
- Bejan, A. (1982). *Entropy Generation through Heat and Fluid Flow*, John Wiley and Sons, USA.
- Bourouaine, S., O. Alexandrova, E. Marsch and M. Maksimovic (2012). On spectral breaks in the power spectra of magnetic fluctuations in fast solar wind between 0.3 and 0.9 au, *The Astrophysical Journal*, 749 (102), 7.
- Boyce, W. E. and R. C. Di Prima (2009). *Elementary Differential Equations and Boundary Value Problems*, 9<sup>th</sup> ed., John Wiley and Sons, Inc., USA.
- Brannigan, L., D. P. Marshall, A. Naveira-Garabato and A. J. G. Nurser (2015). The seasonal cycle of Submesoscale flows, *Ocean Modelling*, 15.
- Brodkey, R. S. (1967), *The Phenomena of Fluid Motions*, Addison-Wesley Publishing Co, USA.
- Brodkey, R. S. and H. C. Hershey (1988). *Transport Phenomena: A Unified Approach*, McGraw-Hill Book Co.
- Bruno, R., D. Telsoni, D. Delure and E. Pietropaulo (2017). Solar wind magnetic field back-ground spectrum from fluid to kinetic scales, *MNRAS*, 472, 1052–1059.
- Calderbank, P. H. and M. B. Moo-Young (1961). The continuous phase heat and mass-transfer properties of dispersions, *Chemical Engineering Science* 16, 39-54.
- Cerbus, R. Y., C. C. Liu, G. Gioia and P. Chakraborty (2020). Small-scale universality in the spectral structure of transitional pipe flows, *Science Advances*, Jan 24; 6(4):eaaw6256.
- Chen, Y. (2019). Simulation and experimental investigation of power consumption, gas dispersion and mass transfer coefficient in a multi-phase stirred bioreactor, *Brazilian Journal of Chemical Engineering*, 36(4), 1439-1451.
- Cheng, X. L., B. L. Wang, F. Hu and R. Zhu (2010). Kolmogorov constants of atmospheric turbulence over a homogeneous surface, *Atmospheric and Oceanic Science Letters*, (3)4, 195-200.
- Chu, C. R. and G. H. Jirka (2003). Wind and Stream Flow Induced Reaeration, *Journal of Environmental Engineering, ASCE* 129(12), 1129-1136,
- Gamard, S. and W. K. George (1999). Reynolds number dependence of energy spectra in the overlap region of isotropic turbulence, *Flow, Turbulence and Combustion* 63, 443–477.
- Goldstein, M. L., R. T. Wicks, S. Perri and F. Sahrroui (2015). Kinetic scale turbulence and dissipation in the solar wind: key observational results and future outlook, *Philosophical Transactions of the Royal Society A* 373: 20140147.
- Hanjalić, K. (2006). *Turbulence and transport phenomena: modelling and simulation*, 150p. [https://www.academia.edu/22152743/TURBULENCE\\_AND\\_TRANSPORT\\_PHENOMENA\\_Modelling\\_and\\_Simulation](https://www.academia.edu/22152743/TURBULENCE_AND_TRANSPORT_PHENOMENA_Modelling_and_Simulation).
- Heisenberg, W. (1948). On the theory of statistical and isotropic turbulence, *Proceedings of the Royal Society*, 402-406.
- Hinze, J. O. (1959). *Turbulence: An Introduction to its Mechanism and Theory*, McGraw-Hill.
- Holland, F. A. and R. Bragg (1995). *Fluid Flows for Chemical Engineers*, 2<sup>nd</sup> ed., Arnold, a division of Hodder Headline PLC, London.
- Hoque, M. M., M. J. Sathe, S. Mitra, I. B. Joshi and G. M. Evans (2015). Comparison of specific energy dissipation rate calculation methodologies utilising 2D PIV velocity measurement, *Chemical Engineering Science* 137, 752–767.
- Kolmogorov, A. N. (1941). The local structure of turbulence in incompressible viscous fluid for very large Reynolds' numbers. *Proceedings of the USSR Academy of Sciences* 30, 301–305.
- Lamont, J. C. and D. Scott (1970). An eddy cell model of mass transfer into the surface of a turbulent liquid, *AIChE Journal* 16(4), 513-519.
- Layton, W. (2018) Turbulence: numerical analysis, modelling and simulation, Special Issue, *Fluids*, MDPI, St. Alban-Anlage 66, Basel, Switzerland, [http://www.mdpi.com/journal/fluids/special\\_issues/turbulence](http://www.mdpi.com/journal/fluids/special_issues/turbulence).
- Lien, R. C. and T. B. Sanford (2001). Turbulence spectra and local similarity scaling in a strongly stratified oceanic bottom boundary layer, *Continental Shelf Research* 24(3), 375-392.
- McComb, W. D. and M. Q. May (2018). The effect of Kolmogorov (1962) scaling on the universality of turbulence energy spectra SUPA School of Physics and Astronomy, University of Edinburgh.
- Monin, A. S. and A. M. Yaglom (1979). *Statistical Fluid Mechanics: Mechanics of Turbulence*, Volume 1, the MIT Press, 4<sup>th</sup> ed.
- Monin, A. S. and A. M. Yaglom (1981). *Statistical Fluid Mechanics: Mechanics of Turbulence*, Volume 2, the MIT Press, 2<sup>th</sup> ed..
- Nature Physics* (2016). Big whorls, little whorls, *Nature Phys* 12, 197, quoting Richardson, L. F. 1922, *Weather Prediction by Numerical Process*. Cambridge University Press.
- Neely, T. W., A. S. Bradley, E. C. Samson, S. J. Rooney, E. M. Wright, K. J. H. Law, R. Carretero-González, P. G. Kevrekidis, M. J. Davis and B. P. Anderson (2013). Characteristics of two-dimensional quantum

- turbulence in a compressible Superfluid, *Physical Review Letters* 111, 235301.
- Obukhov, A. M. (1941). On the distribution of energy in the spectrum of turbulent flow, *Comptes Rendus of the Academy of Sciences of the U.R.S.S* 32, 19.
- Onsager, K. (1945). The distribution of energy in turbulence. *Physical Review*, 68:281.
- Osada, J. (1972). *Evolution of the ideas in physics*, Edgard Blücher Ed., University of São Paulo Ed., (book in Portuguese), Brazil.
- Patankar, S. V. (1980). *Numerical heat transfer and fluid flow*, 1<sup>st</sup> ed., Series in Computational Methods in Mechanics and Thermal Sciences, CRC Press, Taylor and Francis Group, Boca Raton, FL.
- Pope, S. B. (2000). *Turbulent Flows*, Cambridge University Press, 1<sup>st</sup> ed., UK.
- Puga, A. J. (2016). *Characteristics of the velocity power spectrum as a function of Taylor Reynolds number*, PhD thesis for Mechanical and Aerospace Engineering presented at the University of California, Irvine.
- Rebollo, T. C. and R. Lewandowski (2014). Mathematical and numerical foundations of turbulence models and applications, *Series in Modeling and Simulation in Science, Engineering and Technology*, Birkhäuser.
- Rodi, W. (2000). *Turbulence Models and Their Application in Hydraulics A State-of-the-Art Review*, 3<sup>rd</sup> Ed., IAHR, International Association of Hydraulic Research, Monograph Series.
- Saddoughi, S. G. and S. V. Veeravalli (1994). Local isotropy in turbulent boundary layers at high Reynolds number. *J. Fluid Mech.* 268, 333-372.
- Sassa, K. and H. Makita (2005) Reynolds number dependence of elementary vortices in turbulence, Proceedings International Symposium on Engineering Turbulence Modelling and Measurements; ETMM6, Sardinia, Italy, 431-440.
- Schulz, H. E. (1991) *Investigação do mecanismo de reoxigenação da água em escoamento e sua correlação com o nível de turbulência junto à superfície – Parte 2* (Investigation of the reoxygenation mechanism of flowing water and its correlation with the turbulence level at the surface—2<sup>nd</sup> Part, in Portuguese) PhD Thesis, São Carlos School of Engineering, University of São Paulo, São Carlos, Brazil.
- Schulz, H. E. and M. F. Giorgetti (1991). Measurements of reaeration coefficient with the solids probe, In: *Air-water Mass Transfer*, S. C. Williams and J. S. Gulliver (eds), ASCE, 278-293.
- Schulz, H. E. (2001). *Alternatives in Turbulence*, EESC, Printed by University of São Paulo (book in Portuguese, ISBN 8585205377), Brazil.
- Schmitt, F. G. (2017). Turbulence from 1870 to 1920: the birth of a noun and of a concept, *C. R. Mecanique* 345, 620–626.
- Selvi, N. and P. Sugumar (2018) Concepts of thermodynamics, *International Journal of Pure and Applied Mathematics* 119 (12), 1675-1683.
- Slaughter, G. M. (1964). *Investigation of the energy spectrum of turbulence in a closed rectangular conduit*, PhD Thesis, Georgia Institute of Technology, 190p.
- Stewart, S. M. and R. B. Johnson (2016). *Blackbody Radiation: A History of Thermal Radiation Computational Aids and Numerical Methods*, 1<sup>st</sup> Ed., CRC Press, Boca Raton.
- Tung, K. K. (2003). The  $k^{-3}$  and  $k^{-5/3}$  energy spectrum of atmospheric turbulence: Quasigeostrophic Two-Level Model Simulation, *Journal of the Atmospheric Sciences* 60, 824-835.
- Vassilicos, J. C. (2015). Dissipation in turbulent flows, *Annu. Rev. Fluid Mech.*, first published online as a Review in Advance on August 25, 2014, 47, 95–114.
- Verscharen, D., R. T. Wicks, O. Alexandrova, R. Bruno, D. Burgess, C. H. K. Chen, R. D’Amicis, J. D. Keyser, T. D. Wit, L. Franci, J. He, P. Henri, S. Kasahara, Y. Khotyaintsev, K. G. Klein, B. Lavraud, B. M. Maruca, M. Maksimovic, F. Plaschke, S. Poedts, C. S. Reynolds, O. Roberts, F. Sahraoui, S. Saito, C. S. Salem, J. Saur, S. Servidio, J. E. Stawarz, Š. Štverák and D. Told (2021). A Case for electron-astrophysics, *Exp Astron, Voyage 2050-Science themes for ESA’s long-term plan for the science programme: Solar Systems, ours and others (Part2)*.
- Voitenko, Y. and J. De Keyser (2011). Turbulent spectra and spectral kinks in the transition range from MHD to kinetic Alfvén turbulence, *Nonlin. Processes Geophys* 18, 587–597.
- Wang, G., F. Yang, K. Wu, Y. Ma, C. Peng, T. Liu, and L. P. Wang (2021). Estimation of the dissipation rate of turbulent kinetic energy: a review, *Chemical Engineering Science* (229), 116133, 17p.
- White, F. M. (2016). *Fluid Mechanics*, University of Rhode Island, McGraw-Hill Education, NY, USA, 864p.
- Xia, H., N. Francois, H. Punzmann and M. Shats (2013). Lagrangian scale of particle dispersion in turbulence, *Nature Communications*, 4